A Reduced Forward Operator for Acoustic Scattering Problems

Koen W.A. van Dongen[†], Conor Brennan[§] and William M.D. Wright[*]

[†][*] *Ultrasonics Research Group*
Department of Electrical and Electronic Engineering
University College Cork, Cork
IRELAND

[§] *RF Modelling and Simulation Group*
School of Electronic Engineering
Dublin City University, Dublin
IRELAND

E-mail:[†]koen@rennes.ucc.ie [§]brennanc@eeng.dcu.ie [*]bill.wright@ucc.ie

Abstract — **This paper describes the development of a reduced forward operator for solving acoustic scattering problems that arise in ultrasonic imaging applications. The reduction, inspired by the contrast source inversion technique, is obtained by decoupling the interaction between locations in the computational domain at which contrast is present and those positions at which there is a zero contrast. The decoupling is achieved by multiplication by a diagonal matrix whose entries reflect the presence or absence of contrast at the associated point. Numerical results confirm that the reduced operator produces convergent results in less iterations.**

I Introduction

Wave scattering is a fundamental physical process of central importance to a large number of engineering disciplines, such as wireless communications networks, ground penetrating radar, seismic and ultrasonic imaging. Our application area is the use of modeling techniques to support the development of novel clinical ultrasonic imaging techniques and to model hyperthermia cancer treatment by using focussed ultrasound. Practical numerical models of wave scattering have historically required the introduction of judiciously chosen simplifying approximations to keep the computational burden reasonable while producing acceptable results. Included in this class are asymptotic, or ray-based, models. These are computationally tractable but are strictly valid only in the limit of vanishing wavelength and consequently suffer from a variety of related shortcomings. In contrast full-wave models such as those based on the integral equation or differential equation formulation offer numerically exact solutions. A specific advantage of the integral equation formulation is the fact that only the scatterer needs to be discretised. This discretisation can take place on the scatterer surface or within its volume depending on the level of material inhomogeneity the scatterer displays. The use of a suitable Green's function couples the unknown fields together in a compact fashion and removes the need for special treatment of the edges of the computational domain, such as the absorbing boundary conditions used in finite difference techniques [1]. The considerable disadvantage of the integral equation formulation is the computational complexity of their solution. Discretising the integral equation results in a linear system involving N unknowns. The matrix is complex valued and dense, with no zero entries. An iterative solution, such as the method of conjugate gradients (CG), requires $\mathcal{O}(N^2)$ computations per iterative step. There is thus a considerable computational advantage to be had by reducing the number of steps required before satisfactory convergence is reached. This paper presents a novel method for improving the convergence of a conjugate gradient iterative solution of the problem of acoustic wave scattering from an inhomogeneous scatterer whose location and composition are specified. Related, but distinct work, on the inverse problem (where the material composition of the scatterer is not known and must be inferred from measurements of the fields scattered from it at distinct points) is also presented at this conference [2].

The paper is arranged as follows. Section (II) introduces the integral equation formulation for the acoustic scattering case. It also introduces the novel technique for expediting the iterative solution. This involves pre-multiplying both sides of the linear system by a diagonal matrix whose diagonal entries reflect the presence, or lack, of material contrast within the associated basis sub-

domain. Section (III) elaborates on the computational method while section (IV) presents results verifying the method's improved convergence properties when contrasted with a standard CG method.

II Formulation of the Forward Problem

We use the integral equation formulation to describe the scattering problem. This formulation exactly accounts for all wave effects such as reflection, diffraction, refraction and scattering. The formulation is in the temporal Laplace domain with Laplace parameter $\hat{s}$. Frequency domain results are obtained by taking the limit $\hat{s} \rightarrow -i\omega$, with $i^2 = -1$ and ω the temporal angular frequency, where the symbol "$\hat{}$" is used to denote temporal dependency. The vectors x_m or x_n denote positions in the spatial domain $\mathbb{R}^3$, hence $\{m, n\} = 1, 2$ or 3.

Combining reciprocity[3] with the acoustic wave field equations results in an expression for the total pressure wave field $\hat{p}^{\text{tot}}(x_m)$ and the total velocity wave field $\hat{v}_i^{\text{tot}}(x_m)$ for $\{i, j\} = 1, 2$ or 3 in the presence of acoustic contrasts, which reads

$$\hat{p}^{\text{tot}}(x_m) = \hat{p}^{\text{inc}}(x_m) + \hat{p}^{\text{sct}}(x_m)\,, \tag{1}$$

$$\hat{v}_i^{\text{tot}}(x_m) = \hat{v}_i^{\text{inc}}(x_m) + \hat{v}_i^{\text{sct}}(x_m)\,, \tag{2}$$

where $\hat{p}^{\text{inc}}(x_m)$ and $\hat{v}_k^{\text{inc}}(x_m)$ are the incident pressure and velocity wave fields and where $\hat{p}^{\text{sct}}(x_m)$ and $\hat{v}_i^{\text{sct}}(x_m)$ are the scattered pressure and velocity wave fields. These scattered wave fields equal

$$\begin{aligned}\hat{p}^{\text{sct}}(x_m) = {} & \hat{\mathcal{G}}^{pq}(x_m, x_n)\Delta\hat{\eta}(x_n)\hat{p}^{\text{tot}}(x_n) \\ & + \hat{\mathcal{G}}_i^{pf}(x_m, x_n)\Delta\hat{\zeta}(x_n)\hat{v}_i^{\text{tot}}(x_n)\,, \end{aligned} \tag{3}$$

$$\begin{aligned}\hat{v}_i^{\text{sct}}(x_m) = {} & \hat{\mathcal{G}}_i^{vq}(x_m, x_n)\Delta\hat{\eta}(x_n)\hat{p}^{\text{tot}}(x_n) \\ & + \hat{\mathcal{G}}_{i,j}^{vf}(x_m, x_n)\Delta\hat{\zeta}(x_n)\hat{v}_j^{\text{tot}}(x_n)\,, \end{aligned} \tag{4}$$

where the contrast functions $\Delta\hat{\eta}(x_n)$ and $\Delta\hat{\zeta}(x_n)$ are defined by differences between the compressibility κ and volume density ρ of the background medium (bg) and the object medium (obj). Specifically

$$\Delta\hat{\eta}(x_n) = \hat{s}\Delta\kappa(x_n) = \hat{s}\left[\kappa^{\text{bg}} - \kappa^{\text{obj}}(x_n)\right]\,, \tag{5}$$

$$\Delta\hat{\zeta}(x_n) = \hat{s}\Delta\rho(x_n) = \hat{s}\left[\rho^{\text{bg}} - \rho^{\text{obj}}(x_n)\right]\,. \tag{6}$$

The Green's tensor functions shown in equations (3) and (4) are defined as follows

$$\hat{\mathcal{G}}^{pq}(x_m, x_n)\hat{q}(x_n) = \zeta^{\text{bg}}\hat{G}(x_m, x_n) * \hat{q}(x_n)\,, \tag{7}$$

$$\hat{\mathcal{G}}_i^{pf}(x_m, x_n)\hat{f}_i(x_n) = -\partial_i\left[\hat{G}(x_m, x_n) * \hat{f}_i(x_n)\right]\,, \tag{8}$$

$$\hat{\mathcal{G}}_i^{vq}(x_m, x_n)\hat{q}(x_n) = -\partial_i\left[\hat{G}(x_m, x_n) * \hat{q}(x_n)\right]\,, \tag{9}$$

$$\begin{aligned}\hat{\mathcal{G}}_{i,j}^{vf}(x_m, x_n)\hat{f}_j(x_n) = \frac{1}{\zeta^{\text{bg}}}\Big\{ & \\ & \partial_i\partial_j\left[\hat{G}(x_m, x_n) * \hat{f}_j(x_n)\right] \\ & + \delta_{i,j}\delta(x_m - x_n) * \hat{f}_j(x_n)\Big\}\,, \end{aligned} \tag{10}$$

with ∂_i the spatial derivative in the x_i direction, $\delta_{i,j}$ Kronecker's delta function, $\delta(x_m - x_n)$ the impulse response function, $\hat{G}(x_m, x_n)$ the scalar form of the Green's function, $\hat{q}(x_n)$ a volume density of injection rate source and $\hat{f}_j(x_n)$ a volume density of force. Note that, $f(x_m, x_n) * g(x_n)$ refers to a spatial convolution of the functions $f(x_n)$ and $g(x_n)$ over the domain $\mathbb{D}$ enclosing the contrasts. Therefore, equations (1) to (10) constitute integral equations describing the scattering mechanism.

The equations presented above are integral equations describing the behaviour of continuous unknown fields. In order to numerically solve the problem we must impose a suitable discretisation. This is done by dividing the continuous spatial domain, $\mathbb{D}$, into M subdomains, each with associated basis functions describing the unknown field quantities. In our work we use simple subdomain pulse functions described on a regular cubic grid which encloses the scatterers. The use of these basis functions implicitly assumes the wave field to be constant over each subdomain, which must necessarily be small with respect to the wavelength. The imposition of a regular grid is important in that it allows the use of fast Fourier transforms to expedite the computation of fields during the subsequent iterative solution. However, it also means that basis functions are placed at locations where there is no contrast present. Point-matching the fields at points within each subdomain results in a discretised linear system which we describe using tensor notation as

$$\mathsf{p}^{\text{inc}} = \mathsf{p}^{\text{tot}} - Z\mathsf{G}^{pq}\Delta\eta\mathsf{p}^{\text{tot}} - \mathsf{G}^{pf}\Delta\zeta\mathsf{v}^{\text{tot}}\,, \tag{11}$$

$$\mathsf{v}^{\text{inc}} = \mathsf{v}^{\text{tot}} - Z^{-1}\mathsf{G}^{vq}\Delta\eta\mathsf{p}^{\text{tot}} - \mathsf{G}^{vf}\Delta\zeta\mathsf{v}^{\text{tot}}\,, \tag{12}$$

where the constant $Z^2 = \kappa^{\text{bg}}/\rho^{\text{bg}}$ is introduced to normalize the pressure wave field such that the units of the M-dimensional vector p and $3M$-dimensional vector v are identical. Various methods exist to solve this linear system and good results are obtained with the conjugate gradient iterative method[4]. In this scheme, a normalized

error functional Err_n is minimized iteratively. After n iterations, the error functional Err_n reads

$$Err_n = \frac{\|\mathsf{r}_n\|^2}{\|\mathsf{u}^{\mathrm{inc}}\|^2}\,, \tag{13}$$

where the vectors $\mathsf{u}^{\mathrm{inc}}$ and r are given by

$$\mathsf{u}^{\mathrm{inc}} = \begin{pmatrix} \mathsf{p}^{\mathrm{inc}} \\ \mathsf{v}^{\mathrm{inc}} \end{pmatrix}, \qquad \mathsf{r}_n = \begin{pmatrix} \mathsf{r}_n^p \\ \mathsf{r}_n^v \end{pmatrix}. \tag{14}$$

The residual r_n is based on the solutions obtained in the n-th iteration step for $\mathsf{p}_n^{\mathrm{tot}}$ and $\mathsf{v}_n^{\mathrm{tot}}$. Specifically

$$\mathsf{r}_n^{\mathrm{p}} = \mathsf{p}^{\mathrm{inc}} - \mathsf{p}_n^{\mathrm{tot}} + Z\mathsf{G}^{pq}\Delta\eta\mathsf{p}_n^{\mathrm{tot}} + \mathsf{G}^{pf}\Delta\zeta\mathsf{v}_n^{\mathrm{tot}}\,, \tag{15}$$

$$\mathsf{r}_n^{\mathrm{v}} = \mathsf{v}^{\mathrm{inc}} - \mathsf{v}_n^{\mathrm{tot}} + Z^{-1}\mathsf{G}^{vq}\Delta\eta\mathsf{p}_n^{\mathrm{tot}} + \mathsf{G}^{vf}\Delta\zeta\mathsf{v}_n^{\mathrm{tot}}\,. \tag{16}$$

Note that, $\|\mathsf{u}\|^2$ denotes the L_2-norm of a vector u. This norm is defined via the inner product $\langle \mathsf{u}, \mathsf{u}\rangle$ which involves a summation of all the elements of the vector u in the spatial domain $\mathbb{D}$, hence

$$\|\mathsf{u}\|^2 = \langle \mathsf{u}, \mathsf{u}\rangle = \sum \left(\mathsf{p}\mathsf{p}^* + \mathsf{v}\mathsf{v}^*\right)\,, \tag{17}$$

where a * is used to show that the complex conjugate of the vector is taken.

As a consequence of the definition of the forward operator given in equations (11) and (12) and the norm of a vector as shown in equation (17) approximate values for the wave fields are computed everywhere in the spatial domain $\mathbb{D}$. These approximate values are obtained by updating the total wave fields during each iteration step, where the update directions are obtained by applying the adjoint of the forward operator on the residuals. However, from the same set of equations it is observed that the only contribution to the scattered wave fields comes from those positions where there is a non-zero contrast. Fields at points where there is a zero contrast are unknown but do not affect the computation of fields at positions where there is non-zero contrast. The new method exploits this by explicitly decoupling the interaction between fields at positions with zero contrasts and those at positions with non-zero contrasts. This is achieved by introducing a reduced form of the forward operator shown in equations (11) and (12). This reduced forward operator reads

$$\tilde{\mathsf{I}}^p\mathsf{p}^{\mathrm{inc}} = \tilde{\mathsf{I}}^p\left[\mathsf{p}^{\mathrm{tot}} - Z\mathsf{G}^{pq}\Delta\eta\mathsf{p}^{\mathrm{tot}} - \mathsf{G}^{pf}\Delta\zeta\mathsf{v}^{\mathrm{tot}}\right]\,, \tag{18}$$

$$\tilde{\mathsf{I}}^v\mathsf{v}^{\mathrm{inc}} = \tilde{\mathsf{I}}^v\left[\mathsf{v}^{\mathrm{tot}} - Z^{-1}\mathsf{G}^{vq}\Delta\eta\mathsf{p}^{\mathrm{tot}} - \mathsf{G}^{vf}\Delta\zeta\mathsf{v}^{\mathrm{tot}}\right]\,, \tag{19}$$

where $\tilde{\mathsf{I}}$ is a diagonal matrix whose diagonal elements are one or zero depending on the presence or absence of contrast at the associated position in the computational domain. Specifically the diagonal entry corresponding to location (x_m) is given by

$$\tilde{\mathsf{I}}^{p,v}(x_m)\begin{cases} = 1 & \text{for } \Delta\eta(x_m) \neq 0 \text{ or } \Delta\zeta(x_m) \neq 0\,, \\ = 0 & \text{for } \Delta\eta(x_m) = 0 \text{ and } \Delta\zeta(x_m) = 0\,. \end{cases} \tag{20}$$

Note that the limiting situation where the "reduced" identity matrix $\tilde{\mathsf{I}}$ is equal to the identity matrix I corresponds to the case where there is contrast present everywhere in the spatial domain $\mathbb{D}$. In this case, the original form of the forward operator is obtained again and no computational savings are achieved.

Table 1: The conjugate gradient inversion scheme.

$$\tilde{\mathsf{d}}_n = \tilde{\mathsf{G}}^H\tilde{\mathsf{r}}_{n-1} + \frac{\langle \tilde{\mathsf{G}}^H\tilde{\mathsf{r}}_{n-1}, \tilde{\mathsf{G}}^H\tilde{\mathsf{r}}_{n-1} - \tilde{\mathsf{G}}^H\tilde{\mathsf{r}}_{n-2}\rangle}{\left\|\tilde{\mathsf{G}}^H\tilde{\mathsf{r}}_{n-2}\right\|^2}\tilde{\mathsf{d}}_{n-1}$$

$$\tilde{\alpha}_n = \frac{\left\|\tilde{\mathsf{G}}^H\tilde{\mathsf{r}}_{n-1}\right\|^2}{\left\|\tilde{\mathsf{G}}\tilde{\mathsf{d}}_n\right\|^2}$$

$$\tilde{\mathsf{u}}_n^{\mathrm{tot}} = \tilde{\mathsf{u}}_{n-1}^{\mathrm{tot}} + \tilde{\alpha}_n\tilde{\mathsf{d}}_n$$

$$\tilde{\mathsf{r}}_n = \tilde{\mathsf{u}}^{\mathrm{inc}} - \tilde{\mathsf{G}}\tilde{\mathsf{u}}_n^{\mathrm{tot}}$$

$$\widetilde{Err}_n = \frac{\|\tilde{\mathsf{r}}_n\|^2}{\|\mathsf{u}^{\mathrm{inc}}\|^2}$$

$$\mathsf{u}_n^{\mathrm{tot}} = \mathsf{u}^{\mathrm{inc}} + \tilde{\mathsf{u}}_n^{\mathrm{tot}} - \mathsf{G}\tilde{\mathsf{u}}_n^{\mathrm{tot}}$$

$$\mathsf{r}_n = \mathsf{u}^{\mathrm{inc}} - \mathsf{G}\mathsf{u}_n^{\mathrm{tot}}$$

$$Err_n = \frac{\|\mathsf{r}_n\|^2}{\|\mathsf{u}^{\mathrm{inc}}\|^2}$$

III Computational Method

In order to test the reduced form of the forward operator, the conjugate gradient scheme shown in Table 1 was applied. In this scheme, the tensor G^H is the adjoint of the forward operator based on equations (11) and (12). In addition, a ˜ on top of a tensor is used to denote that it is obtained via the reduced form. Hence, it contains only non-zero entries at positions corresponding to locations with non-zero contrast. Note that the table shows the computation of two error functionals; one based on the reduced and one based on the complete form. The latter one is used to compare the results obtained with both methods.

IV Simulation Results and Discussion

The novel numerical method has been tested for a spatial domain with dimensions $4\lambda \times 4\lambda \times 2\lambda$,

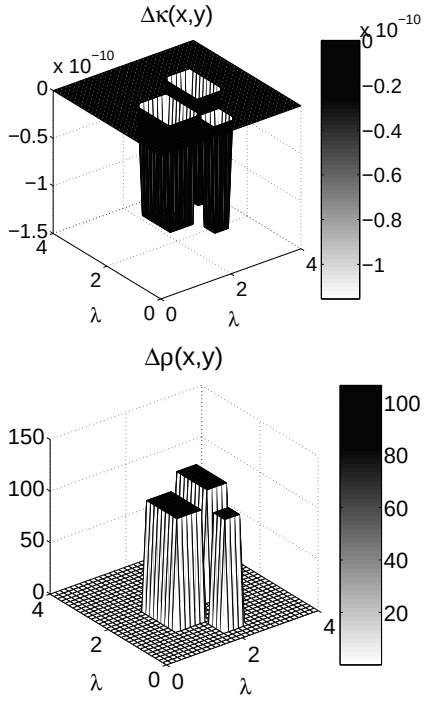

Fig. 1: The contrast function.

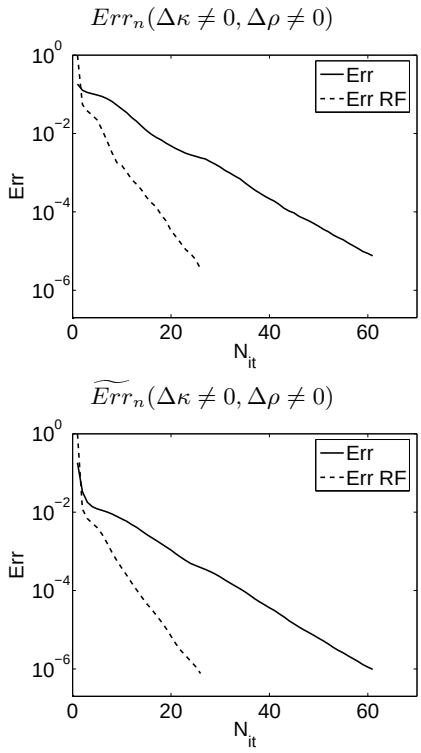

Fig. 2: The error functionals Err (top) and $\widetilde{Err}$ (bottom) for the contrast function shown in Fig. 1. The dashed line refers to the situation where reduced form is applied and solid line where it is not applied. line

with $\lambda = 20$ mm the wavelength of a single frequency probing signal. The volume of each subdomain equals $2.5 \times 2.5 \times 2.5\,\mathrm{mm}^3$. The medium parameters of the background medium correspond to liver tissue, $\kappa^{\mathrm{bg}} = 0.36648\ (\mathrm{G\,Pa})^{-1}$ and $\rho^{\mathrm{bg}} = 1056.6\ \mathrm{kg/m}^3$, while the three objects have medium parameters similar to fat, $\kappa^{\mathrm{obj}} = 0.4819\ (\mathrm{G\,Pa})^{-1}$ and $\rho^{\mathrm{obj}} = 950.0\ \mathrm{kg/m}^3$[5], [6], [7]. The iterative process was considered to have converged once the normalized error functional $\widetilde{Err}$ became smaller than 10^{-6}.

In Fig. 2 the error functionals Err_n (top) and $\widetilde{Err}$ (bottom) are shown for the contrast function shown in Fig. 1. The solid lines refer to the standard situation, given by $\tilde{\mathsf{I}} = \mathsf{I}$, while the dashed line refers to situation where the reduced form is used. Fig. 3 shows results where the same computations have been repeated, but now for the situation where there is either zero contrast in compressibility ($\Delta\kappa = 0$) or zero contrast in density ($\Delta\rho = 0$). Finally, we investigated the effect if there are both contrasts in compressibility and density but not at the same location (see Fig. 4). The results for this case are shown in Fig. 5.

In all cases the results show that applying the reduced form of the forward operator clearly results in a decrease in the number of iterations needed to achieve a desired level of convergence.

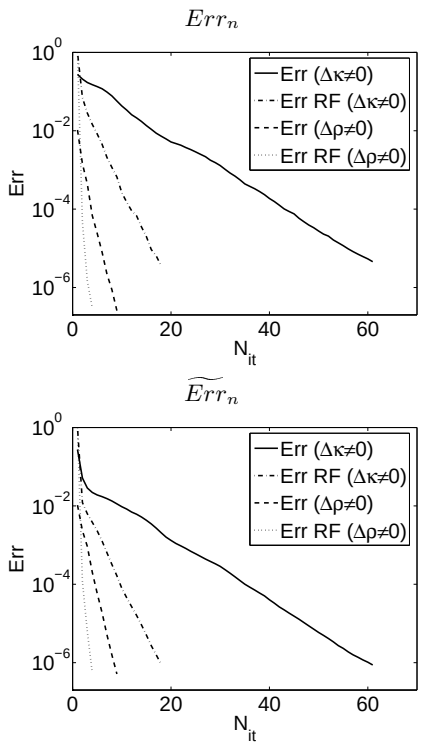

Fig. 3: The error functionals Err (top) and $\widetilde{Err}$ (bottom) in the case where there is either a contrast in the compressibility or in the density.

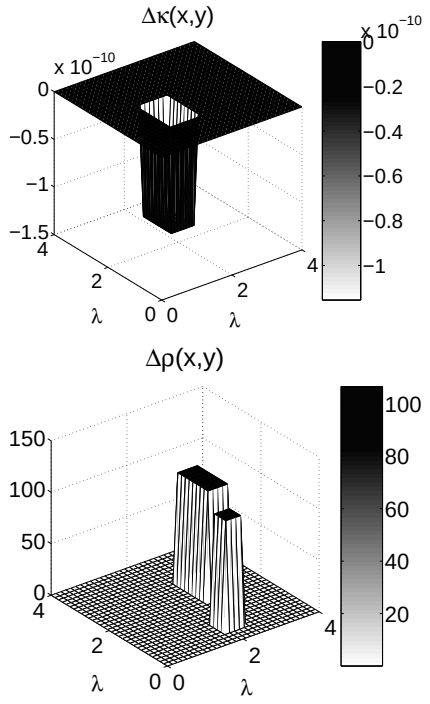

Fig. 4: The contrast function. The location of a contrast in compressibility does not coincide with the location of a contrast in density.

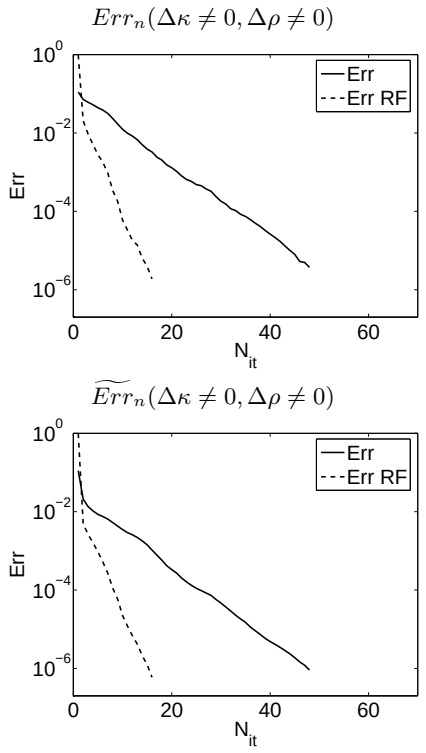

Fig. 5: The error functionals Err (top) and $\widetilde{Err}$ (bottom) for the contrast function shown in Fig. 4.

V Conclusion

This paper has introduced a reduced forward operator for solving the acoustic scattering problems that arise in ultrasonic imaging applications. The reduction is obtained by decoupling the interaction between locations in the computational domain at which contrast is present and those positions at which there is a zero contrast. The decoupling is achieved by multiplication by a diagonal matrix whose entries reflect the presence or absence of contrast at the associated point. Numerical results confirm that the reduced operator produces convergent results in less iterations.

A major advantage of this method as opposed to physically reducing the computational spatial domain is that the same iterative scheme remains valid, independent of the number of scatterers. Hence, we retain the ability to use FFT's to efficiently compute the convolution.

Acknowledgments

This work was financially supported via a Marie Curie Intra-European fellowship.

References

[1] J. P. Berenger, "A perfectly matched layer for the absorption of electromagnetic waves" *J. Comp. Phys.* vol. 114 pp.185-200 1994.

[2] K. Van Dongen and W. Wright, "A contrast source inversion scheme for imaging acoustic contrast" Submitted to *Irish Signals and Systems Conference 2005*

[3] A.T. de Hoop, *Handbook of radiation and scattering of waves: Acoustic Waves in Fluids, Elastic Waves in Solids, Electromagnetic Waves*, Academic Press, London, 1995.

[4] R.E. Kleinman and P.M. van den Berg, "Iterative methods for solving integral equations", *PIERS 5, Application of Conjugate Gradient Method to Electromagnetics and Signal Analysis*, T.K. Sarkar (Ed.), Elsevier, New York, pp. 67–102, 1991.

[5] T.D. Mast, "Empirical relationships between acoustic parameters in human soft tissues", *Acoustics Research Letters Online* vol. 1, no. 2, pp. 37–42, October 2000, and references herein.

[6] N.R. Miller, J.C. Bamber, G.R. ter Haar, "Imaging of temperature-induced echo strain: preliminary in vitro study to assess feasibility for guiding focused ultrasound surgery", *Ultrasound in Medicine and Biology*, vol. 30, no. 3, pp. 345–356, March 2004.

[7] R. Souchon, G. Bouchoux, E. Maciejko, C. Lafon, D. Cathignol, M. Bertrand and

J.Y Chapelon, "Monitoring the formation of thermal lesions with heat-induced echo-strain imaging: a feasibility study", *Ultrasound in Medicine and Biology*, vol. 31, no. 2, pp. 251–259, February 2005.